Large Einstein Radii: A Problem for ΛCDM

(2008, MNRAS, 390, 1647)

Tom J. Broadhurst[1★] and Rennan Barkana[1,2★†]

[1] *Raymond and Beverly Sackler School of Physics and Astronomy, Tel Aviv University, Tel Aviv 69978, Israel*

[2] *Institute for Cosmic Ray Research, University of Tokyo, Kashiwa 277-8582, Japan*

Seminar by **Paramita Barai**

14th Nov, 2008

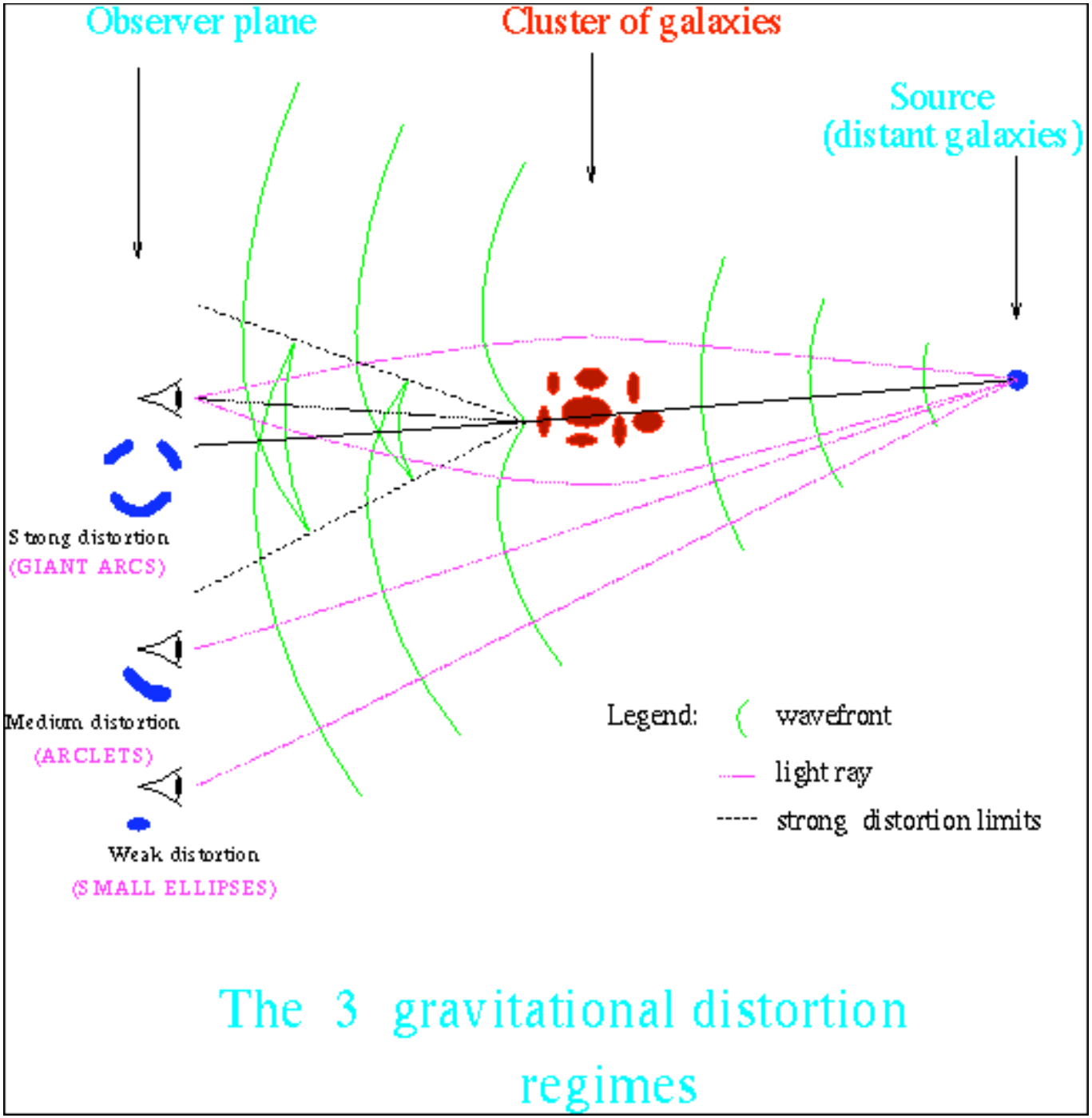

The 3 gravitational distortion regimes

Geometry of Gravitational Lenses

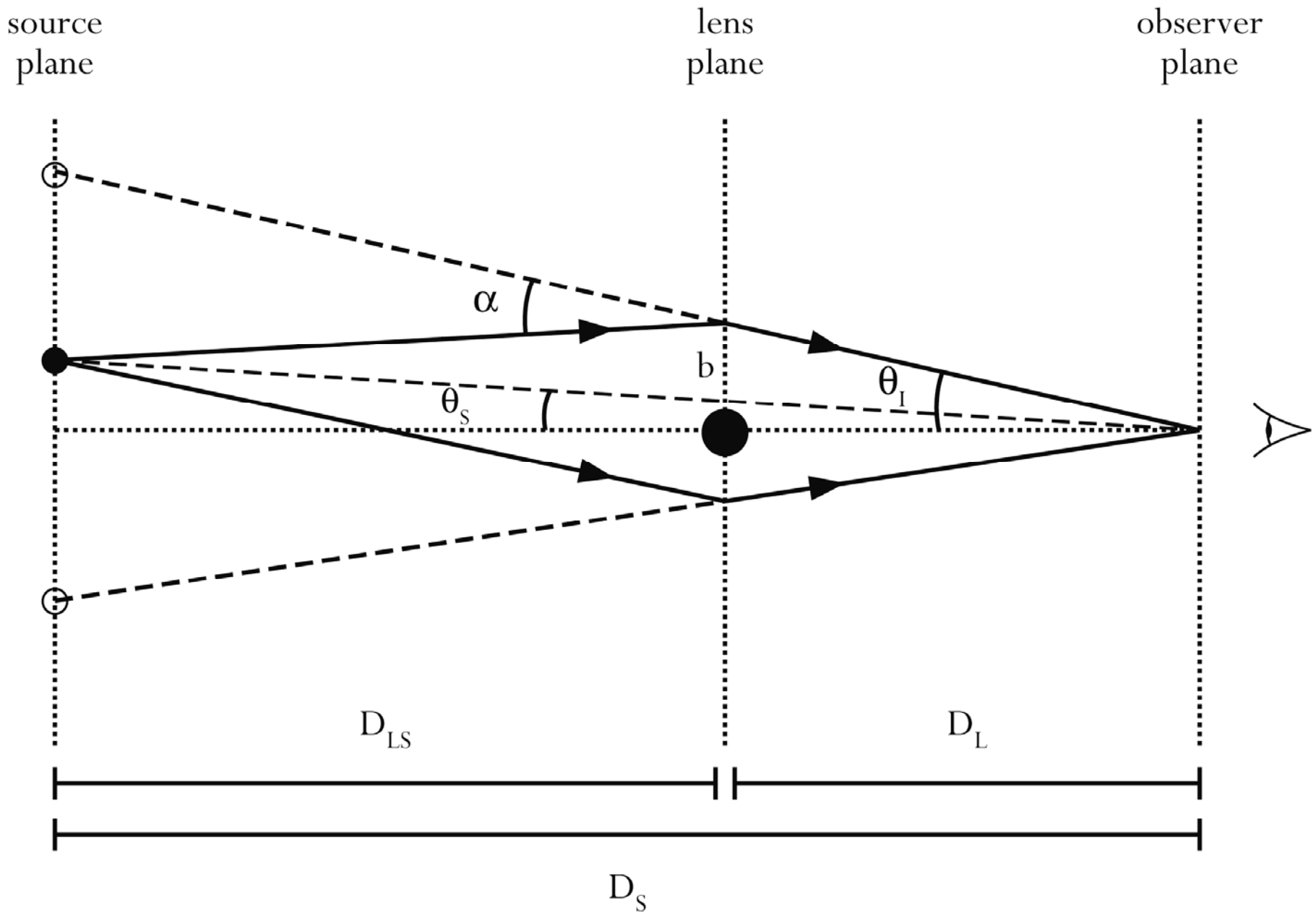

Einstein Ring

- Exact alignment of the source, lens and observer
  - Symmetrical ring-like structure
- Einstein Radius (radians)
  - M = Mass of the lens
  - D = Angular diameter distances

$$\theta_E = \sqrt{\frac{4GM}{c^2}\frac{D_{LS}}{D_L D_S}}$$

- Massive clusters at $0.15 < z < 0.8$
  - $10 < \theta_E < 20$ arcsec
- A1689 : $\theta_E \sim 50$ arcsec

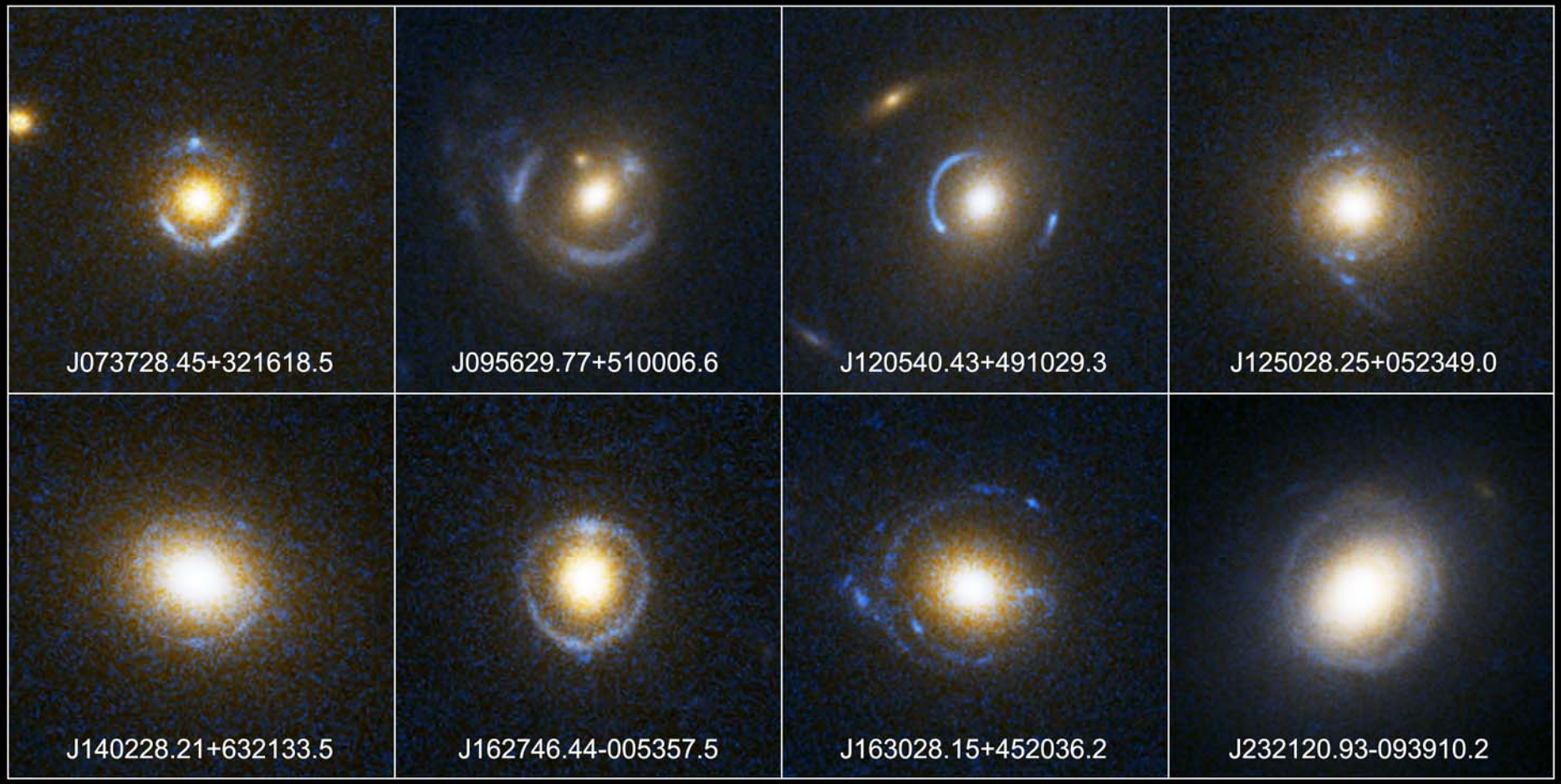

Einstein Ring Gravitational Lenses

Hubble Space Telescope • Advanced Camera for Surveys

NASA, ESA, A. Bolton (Harvard-Smithsonian CfA), and the SLACS Team

STScI-PRC05-32

Standard Cosmology

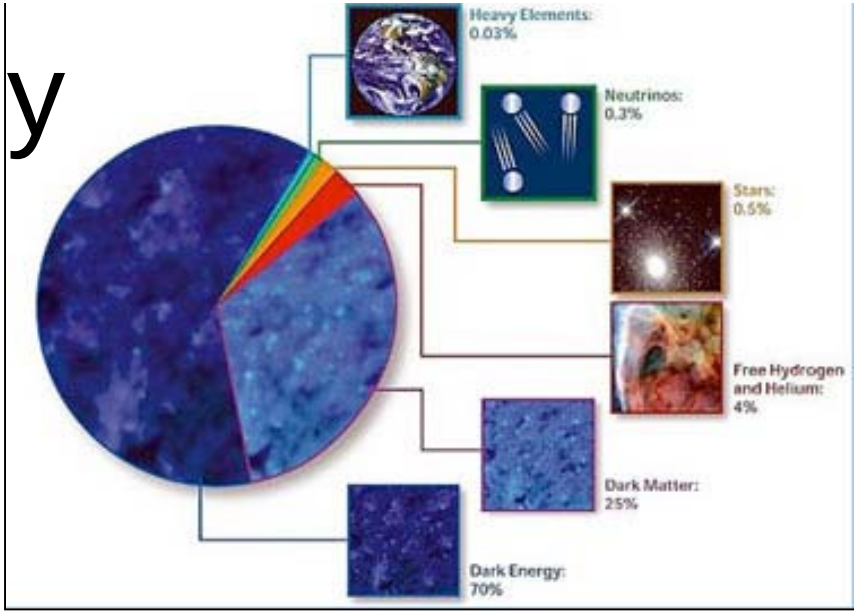

- ΛCDM
- Constrained free parameters

- Empirical evidence
  - CMBR (WMAP), SN data, clustering of galaxies (large surveys: SDSS), gravitational lensing, galaxy cluster abundances
- Dark matter
  - Gravity-only, initially sub-relativistic, initial density perturbations are Gaussian in amplitude
- Non-linear structure growth, affected by gas physics
- Galaxy clusters are excellent probes:
  - Large, massive, gravity-dominated, high-temperature of ICM, no cooling

Overview

- Gravitational lensing observations ⇒ mass profile of galaxy clusters
- Einstein radius ⇒ model independent determination of central mass density

$$M(<\theta_E) = \theta_E^2 \frac{c^2}{4G} \frac{D_L D_S}{D_{LS}}$$

- Authors compare cluster observations with predictions of ΛCDM cosmological simulations
- Compare projected 2D mass/density distributions using
  - Virial mass (*M*)
  - Einstein radius (θ_E)

Theory

$$\rho(r) = \rho_c^z \frac{\delta_c}{\frac{r}{r_s}\left(1+\frac{r}{r_s}\right)^2}$$

- NFW density profile
  - Navarro, Frenk & White 1997, ApJ, 490, 493
- r_s = NFW scale radius = r_{vir}/c_{vir}
- c_{vir} = Concentration parameter

$$\delta_c = \frac{\Delta_c}{3} \frac{c_{vir}^3}{\ln(1+c_{vir}) - \frac{c_{vir}}{1+c_{vir}}}$$

- Δ_c = Overdensity (= 200)
- Parameters: M (halo mass), z (redshift), Δ_c, c_{vir}

Simulated Cluster Samples

- 2 studies of halo structure in cosmological numerical simulations
- Statistical analysis of cluster halo population

Neto et al. 2007

(MNRAS, 381, 1450)

- Millennium simulation
- > 2000 haloes
  - $M_{200} > 10^{14}\ M_{\odot}$
  - $z = 0$
- Each halo resolved with >80,000 particles
- 3-D density structure using NFW profile fitting

Hennawi et al. 2007

(ApJ, 654, 714)

- 900 simulated cluster haloes at $z = 0.41$
- Each resolved with >30,000 particles
- 3-D and projected 2-D NFW profiles
  - Projections thru avg. 15 random directions
- Lensing population
  - Haloes weighted by strong lensing cross-section

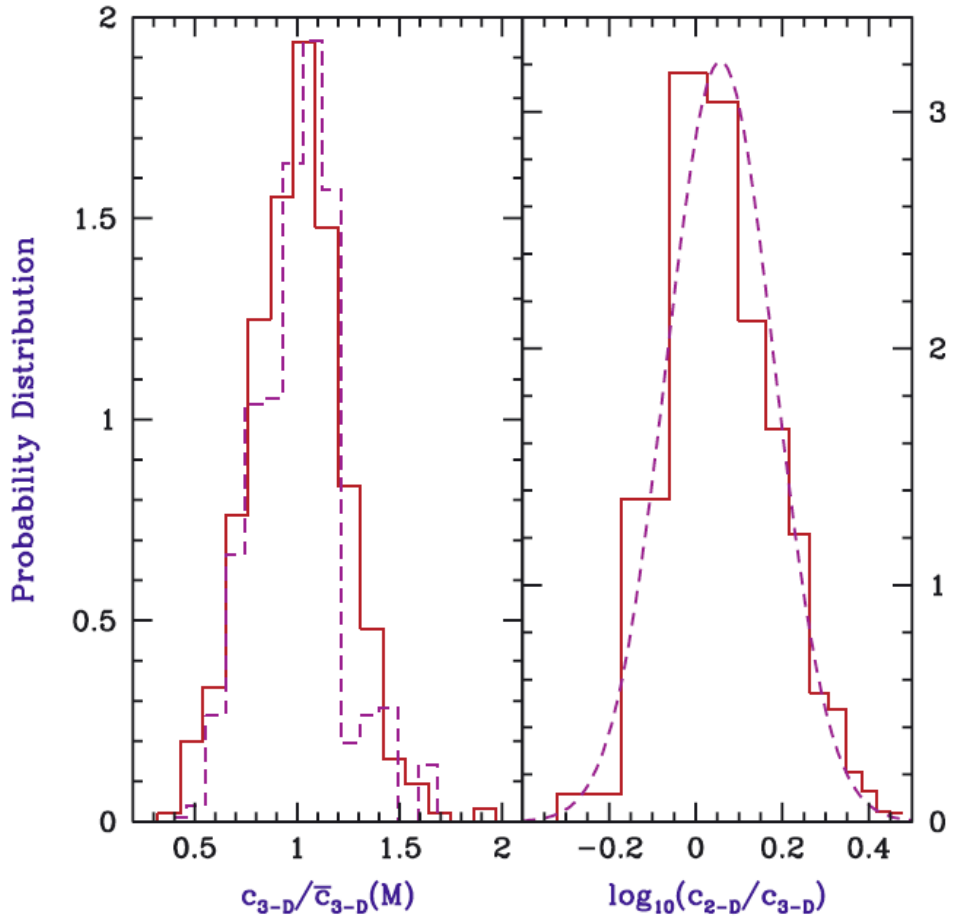

Figure 1. Probability distributions of various concentration parameters, based on Hennawi et al. (2007). Left-hand panel: when the concentration parameters are measured relative to the median at each halo mass (fig. 8 of Hennawi et al. 2007), the distribution for the general population (solid histogram) matches that for the lens population when the latter is divided by a factor of 1.17 (dashed histogram). Right-hand panel: for lensing haloes, the distribution of $\log_{10}$ of the ratio of the 2D to the 3D concentration (solid histogram) is well fitted by a Gaussian with the same mean and variance as the histogram (dashed curve). Note that the non-uniform binning is a result of our conversion of the linear-axis histogram from fig. 12 of Hennawi et al. (2007) to one with a logarithmic x-axis.

Results of Analyses of Numerical Samples

- Halo structure expressed in terms of NFW concentration parameter (c)

Fig. 1 ⇒

1) Distribution of 3-D concentrations of lens population is the same as the general halo population, except for a up-shift by a factor 1.17
2) 2-D projected c's correlate with 3-D c
   - Ratio $c_{2D}/\ c_{3D}$ is lognormal
   - $\log_{10}(c_{2D}/\ c_{3D})$ is well-fitted by Gaussian with mean = 0.057 and std-dev = 0.124

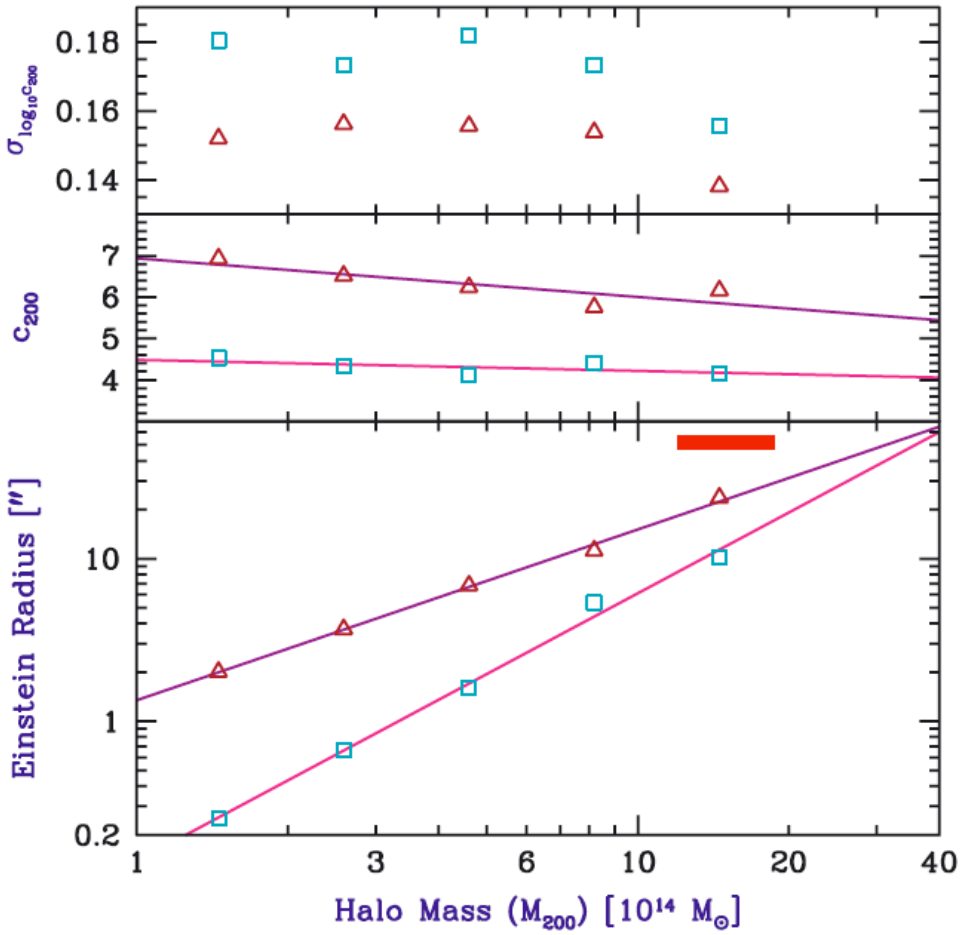

Figure 2. Dependence of θ_E (bottom panel), the median c_{200} (middle panel) and the scatter $\sigma_{\log_{10}c_{200}}$ (top panel) on halo mass M_{200} in numerical simulations. We use the 3D analysis by Neto et al. (2007) corrected for lensing and projection bias based on Fig. 1. We consider the relaxed (triangles) or unrelaxed (squares) halo populations. We assume the median c_{200} and the A1689 redshifts when calculating r_E. We show several linear least-squares fits to help discern trends (solid curves). Also shown for comparison (narrow box, bottom panel) is the location corresponding to the observations of A1689 (where the boxed area contains the two-sided 1σ ranges of M_{200} and θ_E).

Numerical Results

Fig. 2 $\Rightarrow$

- c is higher for relaxed haloes than for unrelaxed (dynamically disturbed ones)

- $c \downarrow$ slowly with halo mass
  - Predicted $\theta_E \propto M_{200}$ (relaxed)
  - Predicted $\theta_E \propto (M_{200})^{1.6}$ (unrelaxed)

Observational Data

- 4 well-studied clusters
  - Strong-lensing: Multiply imaged arcs
  - Weak-lensing: Distorted arcs, magnification
- HST/ACS imaging of lensing clusters by ACS/GTO team (Ford et al. 1998, Proc. SPIE. 3356, 234)
  - Other lensing studies --- CFHT, Subaru
- Many sets of multiple images

  $\Rightarrow$ Fit 2-D projected mass distribution

  $\Rightarrow$ Determine effective Einstein radius
- 3 clusters : Virial mass from NFW fits to lensing observations
- A1689 : Model-independent mass from lensing data (only assuming spherical symmetry)

Data Set of 4 Lensing Clusters

Table 1. Observational data.

Cluster	$M_{\rm vir}$ ($M_\odot$)	M_{200} ($M_\odot$)	$\theta_{\rm E}$ (arcsec)	$z_{\rm L}$	$z_{\rm S}$
A1689	1.6×10^{15}	1.5×10^{15}	52	0.183	3
Cl0024−17	8.7×10^{14}	8.0×10^{14}	31	0.395	1.7
A1703	1.0×10^{15}	9.0×10^{14}	32	0.258	2.8
RXJ1347	1.3×10^{15}	1.2×10^{15}	35	0.45	1.8

Confronting ΛCDM with Observations

- For each cluster find ΛCDM predicted θ_E using z_L, z_S and M_{200}
- Fig. 3 - compares median expected value with observed value

Cluster	Observed θ_E ($''$)	Predicted θ_E ($''$)	Agreement Probability
A1689	52	24	8.5
Cl0024-17	31	15	3.9
A1703	32	16	7.9
RXJ1347	35	23	13

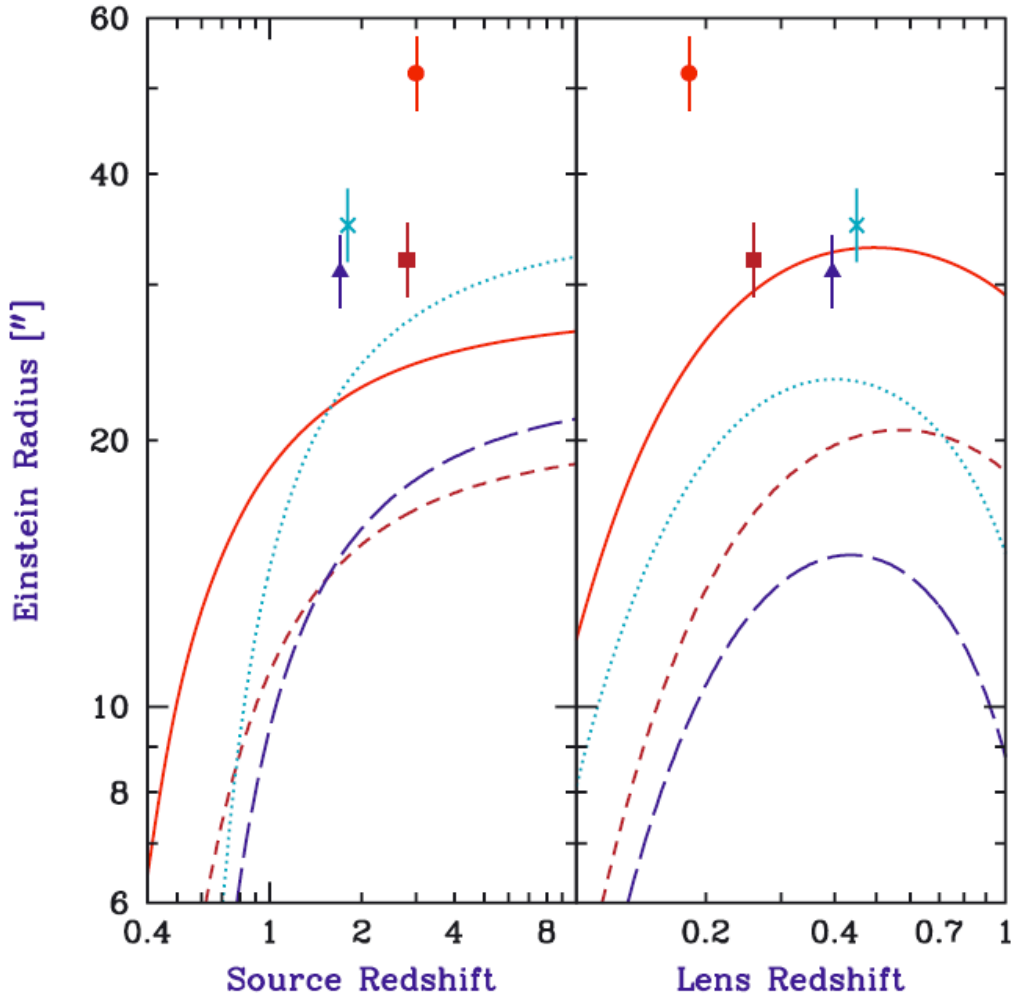

Figure 3. Dependence of the Einstein radius θ_E on the redshifts z_S (left-hand panel) and z_L (right-hand panel). We consider A1689 (solid curves, circles), A1703 (short-dashed curves, squares), Cl0024 (long-dashed curves, triangles) and RX J1347 (dotted curves, $\times$s). In each case, the points correspond to the observed cluster (with a vertical bar indicating the measurement error), while the curves show the predicted θ_E based on the median c_{200} of relaxed simulated haloes as measured by Neto et al. (2007) in the nearest mass bin, after correction for lensing and projection bias based on Fig. 1.

Statistical Comparison

- Fig. 4 $\Rightarrow$ full predicted probability distribution of θ_E for each cluster
- Main predictions give probabilities of 1.5, 0.56, 5.0 and 3.7 % for finding a cluster with a large θ_E as observed
- If just 1 cluster $\Rightarrow 2\sigma$ discrepancy
- But have 4 independent objects
  - All discrepant in the same direction
- Total probability = 3×10^{-5}, that theory would predict such large θ_E for 4 clusters

  $\Rightarrow 4\sigma$ discrepancy

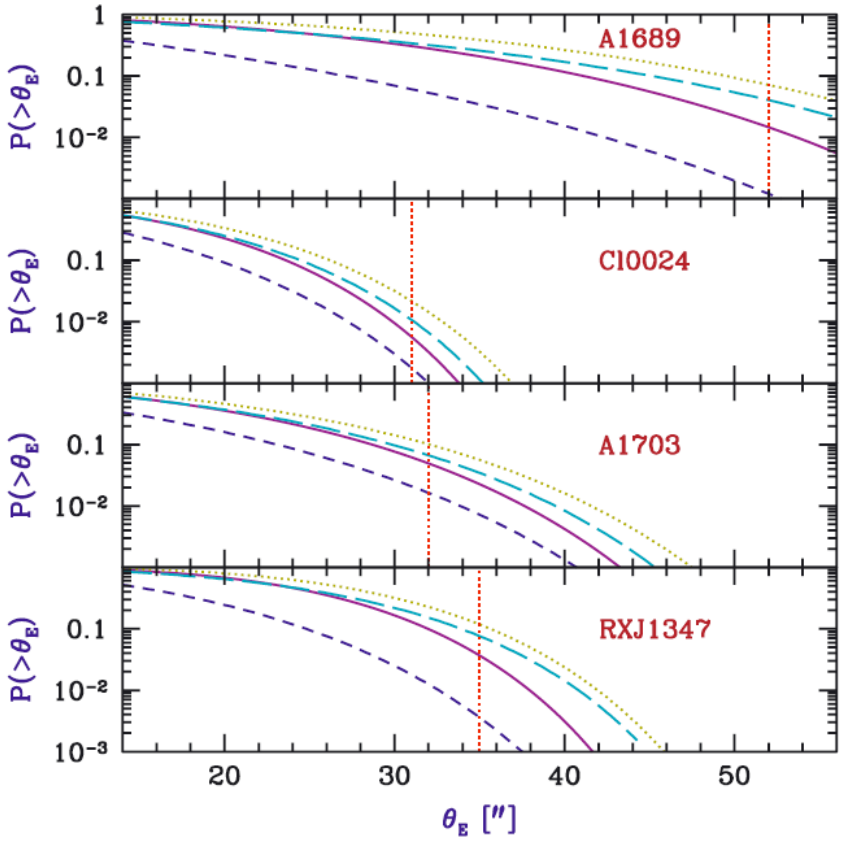

Figure 4. Cumulative probability distribution $P(>\theta_{\rm E})$, assuming the log-normal c_{200} distribution measured by Neto et al. (2007) for haloes from a numerical simulation. We consider A1689, Cl0024, A1703 and RX J1347 as indicated, assuming in each case the best-fitting mass from observations, and the c_{200} distribution as measured from the simulation for the nearest mass bin of relaxed haloes (solid curves). We also consider several possible sources of statistical or systematic error, and we illustrate the result of assuming a cluster mass higher by the 1σ measurement error (dotted curves), or a scatter $\sigma_{\log_{10}c_{200}}$ higher by the 1σ sampling noise (see text; long-dashed curves). In all cases shown, $P(>\theta_{\rm E})$ for unrelaxed haloes would lie below the corresponding curve for relaxed haloes, throughout the plotted region. Thus, we only illustrate the main case with the c_{200} distribution as measured for unrelaxed haloes (short-dashed curves). Also shown for comparison for each cluster (dotted vertical line) is the observed $\theta_{\rm E}$.

Possible Reasons for Discrepancy

- Lensing observations of larger cluster samples
- Theoretically predicted triaxiality of CDM halos $\Rightarrow$ a scatter in projected *c* and θ_E
  - Must determine the scatter observationally
- Observed cluster halos are more centrally concentrated than ΛCDM prediction

  $\Rightarrow$ additional (unknown?) mechanism that causes cluster to collapse/form earlier
  - Adiabatic compression needs a baryon fraction 2 times the cosmic value, $\therefore$ unlikely
- Non-Gaussianity of primordial density fluctuations

Clusters observed with masses ~10^{15} $M_\odot$ are consistent with Λ CDM model

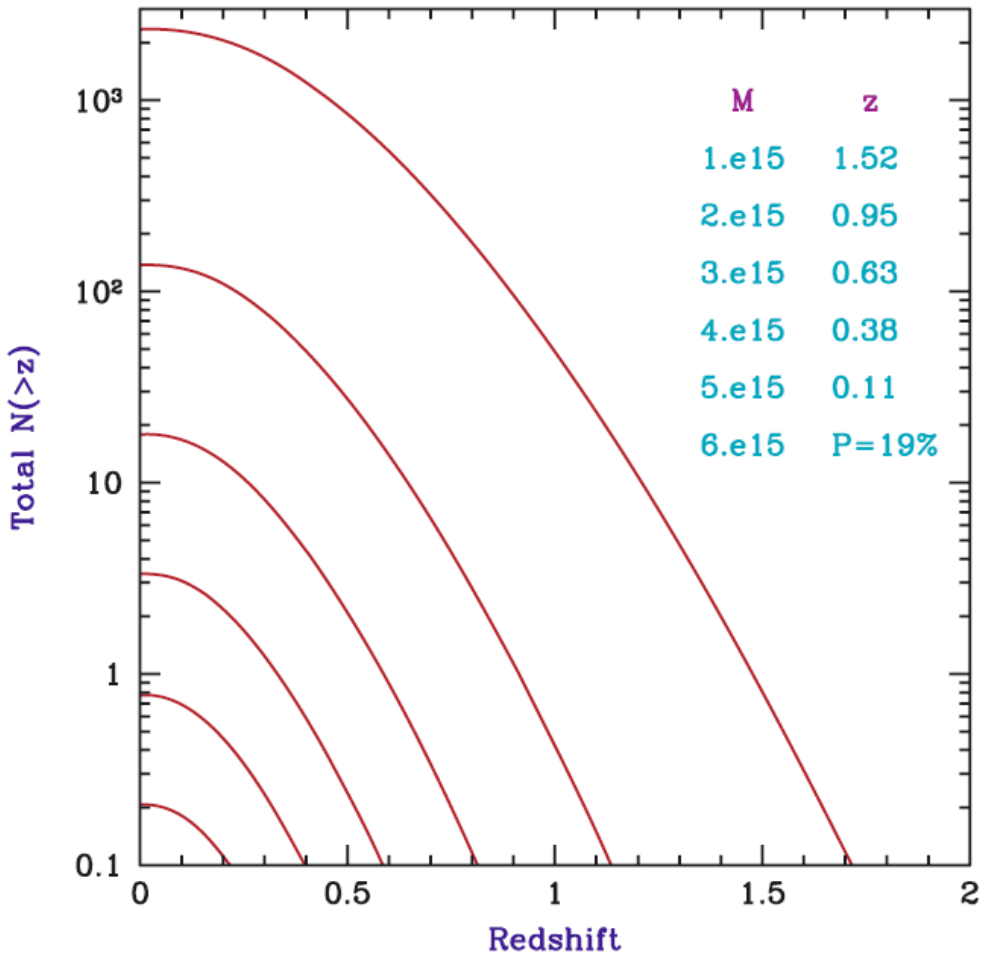

Figure 5. Total number of observable clusters in the universe above redshift z, obtained by integrating the halo mass function of Sheth, Mo & Tormen (2001) over our past light cone. We consider all cluster haloes above virial mass $M = 1, 2, 3, 4, 5$ or 6×10^{15} $M_\odot$ (top to bottom). Also listed for each M (top right-hand corner) is the redshift above which there is a 50 per cent chance of observing at least one halo of mass greater than M. For $M = 6 \times 10^{15}$ $M_\odot$ we instead list the probability of observing at least one halo at any $z > 0$.

Summary

- Compared theoretical predictions vs. observations of θ_E for 4 clusters
- Observed θ_E is large by factor of ~2 w.r.t. ΛCDM model

- " … perhaps the clearest, most robust current conflict between observations and the standard ΛCDM model … "
- " … highly significant discrepancy we have identified already represents a substantial challenge for ΛCDM … "

- Lensing properties of larger cluster halo samples must be studied

Backup